Improvement of Galilean refractive beam shaping system for accurately generating near-diffraction-limited flattop beam with arbitrary beam size

Haotong Ma,* Zejin Liu, Pengzhi Jiang, Xiaojun Xu, and Shaojun Du

College of opto-electronic Science and Engineering, National university of Defense Technology, Changsha, Hunan, 410073, China
*mahaotong@163.com

Abstract: We propose and demonstrate the improvement of conventional Galilean refractive beam shaping system for accurately generating near-diffraction-limited flattop beam with arbitrary beam size. Based on the detailed study of the refractive beam shaping system, we found that the conventional Galilean beam shaper can only work well for the magnifying beam shaping. Taking the transformation of input beam with Gaussian irradiance distribution into target beam with high order Fermi-Dirac flattop profile as an example, the shaper can only work well at the condition that the size of input and target beam meets $R_0 \geq 1.3 w_0$. For the improvement, the shaper is regarded as the combination of magnifying and demagnifying beam shaping system. The surface and phase distributions of the improved Galilean beam shaping system are derived based on Geometric and Fourier Optics. By using the improved Galilean beam shaper, the accurate transformation of input beam with Gaussian irradiance distribution into target beam with flattop irradiance distribution is realized. The irradiance distribution of the output beam is coincident with that of the target beam and the corresponding phase distribution is maintained. The propagation performance of the output beam is greatly improved. Studies of the influences of beam size and beam order on the improved Galilean beam shaping system show that restriction of beam size has been greatly reduced. This improvement can also be used to redistribute the input beam with complicated irradiance distribution into output beam with complicated irradiance distribution.

©2011 Optical Society of America

OCIS codes: (140.3300) Laser beam shaping; (120.5060) Phase modulation; (220.2740) Geometric optical design; (070.0070) Fourier optics and signal processing.

References and links

1. F. M. Dickey, S. C. Holswade, and D. L. Shealy, eds., *Laser Beam Shaping Applications* (CRC Press, 2005).
2. J. A. Hoffnagle and C. M. Jefferson, "Design and performance of a refractive optical system that converts a Gaussian to a flattop beam," Appl. Opt. **39**(30), 5488–5499 (2000).
3. D. L. Shealy and J. A. Hoffnagle, "Laser beam shaping profiles and propagation," Appl. Opt. **45**(21), 5118–5131 (2006).
4. P. W. Rhodes and D. L. Shealy, "Refractive optical systems for irradiance redistribution of collimated radiation: their design and analysis," Appl. Opt. **19**(20), 3545–3553 (1980).
5. M. Arif, M. M. Hossain, A. A. S. Awwal, and M. N. Islam, "Two-element refracting system for annular Gaussian-to-Bessel beam transformation," Appl. Opt. **37**(19), 4206–4209 (1998).
6. J. J. Kasinski and R. L. Burnham, "Near-diffraction-limited laser beam shaping with diamond-turned aspheric optics," Opt. Lett. **22**(14), 1062–1064 (1997).
7. B. R. Frieden, "Lossless conversion of a plane laser wave to a plane wave of uniform irradiance," Appl. Opt. **4**(11), 1400–1403 (1965).
8. C. C. Aleksoff, K. K. Ellis, and B. D. Neagle, "Holographic conversion of a Gaussian-beam to a near-field uniform beam," Opt. Eng. **30**(5), 537–543 (1991).

9. J. H. Li, K. J. Webb, G. J. Burke, D. A. White, and C. A. Thompson, "Design of near-field irregular diffractive optical elements by use of a multiresolution direct binary search method," Opt. Lett. **31**(9), 1181–1183 (2006).
10. G. Zhou, X. Yuan, P. Dowd, Y. L. Lam, and Y. C. Chan, "Design of diffractive phase elements for beam shaping: hybrid approach," J. Opt. Soc. Am. A **18**(4), 791–800 (2001).
11. J. M. Auerbach and V. P. Karpenko, "Serrated-aperture apodizers for high-energy laser systems," Appl. Opt. **33**(15), 3179–3183 (1994).
12. S. Zhang, G. Neil, and M. Shinn, "Single-element laser beam shaper for uniform flat-top profiles," Opt. Express **11**(16), 1942–1948 (2003).
13. S. Zhang, "A simple bi-convex refractive laser beam shaper," J. Opt. A, Pure Appl. Opt. **9**(10), 945–950 (2007).
14. C. Liu and S. Zhang, "Study of singular radius and surface boundary constraints in refractive beam shaper design," Opt. Express **16**(9), 6675–6682 (2008).
15. H. T. Ma, P. Zhou, X. L. Wang, Y. X. Ma, F. J. Xi, X. J. Xu, and Z. J. Liu, "Near-diffraction-limited annular flattop beam shaping with dual phase only liquid crystal spatial light modulators," Opt. Express **18**(8), 8251–8260 (2010).
16. H. T. Ma, Z. J. Liu, P. Zhou, X. L. Wang, Y. X. Ma, and X. J. Xu, "Generation of flat-top beam with phase-only liquid crystal spatial light modulators," J. Opt. **12**(4), 045704 (2010).
17. J. L. Kreuzer, "Coherent light optical system yielding an output beam of desired intensity distribution at a desired equiphase surface," U.S. patent 3,476,463 (4 November 1969).
18. J. W. Goodman, *Introduction to Fourier Optics*, 3rd ed. (Roberts & Company Publishers, 2005).

1. Introduction

Laser beam can only have typical irradiance distributions due to the restriction of laser cavity and gain distribution [1]. However, laser beams with desired irradiance distributions are often required to improve the efficiency in practical applications. For example, uniform irradiance distributions over the cross section are required in the fields of micromachining, laser welding, isotope separation, laser printing, optical processing, laser radars, and efficient power extraction in laser amplifiers [1–16].

In the past decades, a number of techniques and systems, which include by using amplitude and phase filtering elements, are developed to redistribute the irradiance of the input beam. Compared with amplitude filtering method, the phase filtering method by using refractive or diffractive optical element has high conversion efficiency and can be used for high power laser beam shaping [1–16]. As one kind of phase filtering beam shaping system, the refractive beam shaping system with aspheric lenses have been widely studied due to the simple design procedure. The dual aspheric lenses and single aspheric lens configuration for beam shaping has been proposed and studied [1–7,12–14]. According to the working principle, refractive beam shaping system can be divided into two categories: Galilean and Keplerian beam shaping system. Compared with the latter, the Galilean beam shaper is a magnifying beam shaping system and does not contain real focus in beam shaping, so the Galilean beam shaper is more suitable for high power laser beam shaping. In addition, because the surface and phase distributions of Galilean shaping system are smaller than that of the Keplerian shaping system, Galilean beam shaper is more suitable for beam shaping with dual deformable mirrors or spatial light modulators by loading the aspheric lenses' phase distributions [15,16]. However, compared with the Galilean shaping system, the Keplerian shaping system has monotonic and convex surface, which is considerably simpler to fabrication than the Galilean shaping system.

In Ref. [14], S. Zhang and his associate report the "singularity" in solution of the surface profile equations of the Galilean shaping system. Changing the sizes of input and target beam can be used to avoid "singularity". It should be noted that the "singularity" mentioned in Ref. 14 is about solving the surface profile equations and defined in mathematics, but not just implying a physical effect. However, the influences of beam size and beam order on beam shaping effect (irradiance and phase distributions of the output beam) and how to eliminate the influences have not been considered in their work. Unfortunately, sizes of the input and target beam cannot be changed in many applications. In this paper, influences of irradiance distribution of the target beam on beam shaping have been studied in detail. The results show that the conventional Galilean beam shaping system can only work well for the magnifying beam shaping (The size of the target beam is much larger than that of the input beam.). In order to overcome this shortcoming, we propose and demonstrate an improvement of the conventional Galilean shaping system. For the improvement, the shaping system is regarded

as the combination of magnifying and demagnifying beam shaping systems. This improved Galilean shaping system can be used to accurately redistribute input beam with arbitrary beam size into output beam with arbitrary beam size. The restriction of beam size on Galilean beam shaping system has been greatly reduced. To the best of our knowledge, the improvement of Galilean shaping system proposed in this paper has never been reported.

This paper is organized as follows. In the second section, the working principle of dual aspheric lenses beam shaping system and influence of irradiance distribution of the target beam on beam shaping are given. The third section reports the improvement of Galilean beam shaping system and gives the corresponding numerical analysis. In the fourth section, the conclusions are given.

2. Analysis of the conventional Galilean beam shaping system

The basic principle of the refractive beam shaping system is shown in Fig. 1. The working procedure is that the first aspheric lens redistributes the irradiance of the input beam to the desired distribution at the second aspheric lens plane and the second aspheric lens re-collimates the output beam. The shaping system can be treated as an anamorphic variant of beam expanding telescope. After passing through the refractive beam shaping system, the beam with desired irradiance distribution and plane wave front can be realized. According to the working principle, the refractive shaping system can be divided into two categories: Galilean and Keplerian beam shaping systems. The principles are shown in Figs. 1(a) and 1(b) [2,17].
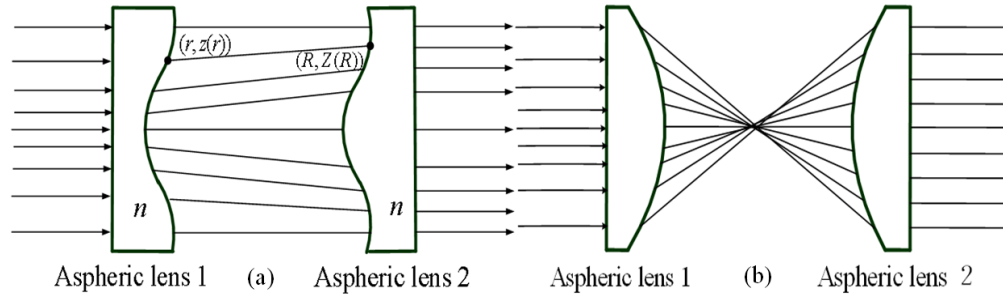

Fig. 1. Configuration of the refractive beam shaping system, (a). Galilean system; (b) Keplerian system.

According to the treatment of Kreuzer [17], relationship between surface distribution and radial position in Galilean beam shaping system can be given by

$$z(r) = \int_0^r \left\{ (n^2 - 1) + \left[\frac{(n-1)d}{h(x) - x} \right]^2 \right\}^{-1/2} dx \qquad (1)$$

and

$$Z(R) = \int_0^R \left\{ (n^2 - 1) + \left[\frac{(n-1)d}{h^{-1}(x) - x} \right]^2 \right\}^{-1/2} dx, \qquad (2)$$

where $z(r)$ is the sag of the first aspheric lens at radial position r, $Z(R)$ is the sag of the second aspheric lens at radial position R, d is the distance between two aspheric lenses, n is the refractive index. $R = h(r)$ and $r = h^{-1}(R)$ are the relationships between the input position at the first aspheric lens and the output position at the second aspheric lens, which can be obtained by using energy conservation principle. According to Fourier Optics, we can get the relationship between the surface and phase distribution in Galilean beam shaping system, which is shown in Eqs. (3) and (4) [15,16].

$$f_{phase1}(r) = \frac{2\pi\left[z_{edge} - z(r) + nz(r)\right]}{\lambda} \tag{3}$$

and

$$f_{phase2}(R) = \frac{2\pi\left[nZ_{edge} - nZ(R) + Z(R)\right]}{\lambda}, \tag{4}$$

where z_{edge} and Z_{edge} denote the edge sags of the first and second aspheric lenses, λ represents the wavelength. In the following sections, we will give studies on conventional Galilean beam shaping system. In numerical simulation, the input and target beams are chosen as the Gaussian and high order Fermi-Dirac profile flattop beams respectively. That is

$$P_{input}(r) = \exp\left(\frac{-2r^2}{w_0^2}\right) \tag{5}$$

and

$$P_{output}(r) = \left\{1 + \exp\left[\beta\left(\frac{r}{R_0} - 1\right)\right]\right\}^{-1}, \tag{6}$$

where w_0 is the beam waist, β is a dimensionless parameter and determines the range over, which the irradiance rolls off exponentially, R_0 is the radius at which the irradiance has fallen to half of its value on axis. For the sake of simplicity and consistency, only one parameter is changed in the following discussion. Numerical simulations are based on the MATLAB. In addition, the angular spectrum method combined with MATLAB is used for modeling the propagation of the input beam [18].

2.1 Influence of target beam size (R_0)

Because the surface and phase distributions of dual aspheric lenses are related with the ratio of the target beam size to the input beam size, we focus on the influence of target beam size (R_0). In simulation, the parameters are selected as $w_0 = 3mm$, $\beta = 16$, $d = 350mm$, $n = 1.45$ and $\lambda = 1064nm$. Based on Eqs. (5), (6) and the energy conversation principle, we can get the relationship $R = h(r)$ and $r = h^{-1}(R)$. From Eqs. (1) and (2), we can see that the point $R = r$ is a singularity and we cannot obtain the analytical solution of the surface profile distribution at this point. In simulation, numerical discrete method is used. In the present and following analysis, the surface profile of the discrete point proximate the singular point is used to represent the surface profile of the singular point. From the following analysis, we can found that the point $R = r$ is not only a singularity, but also the point of inflexion of the phase distribution curve. Figure 2 shows the phase distributions of dual aspheric lenses for the transformation of input beam into target beam with different size (R_0). There exists point of inflexion on the phase distribution curve and the point of inflexion moves outside along with the increase of target beam size (R_0). The corresponding irradiance and phase distributions of the output beam along with the change of target beam size are shown in Figs. 3(a) and 3(b). According to Figs. 3(a) and 3(b), it can be found that the larger the target beam size (R_0) results in smaller difference between output beam and target beam. The flattop area of phase distribution of the output beam becomes larger and larger with the increase of target beam size. In order to give a quantitative analysis of shaping effect, the shaping error between the output beam and target beam is defined as

$$Error = \sqrt{\iint\left[I_{output}(x,y) - I_{target}(x,y)\right]^2 dxdy}, \tag{7}$$

where $I_{output}(x,y)$ and $I_{t\arg et}(x,y)$ are irradiance distributions of output beam and target beam respectively. The change of the shaping error along with the size of the target beam is shown in Fig. 4(a). The increase of the target beam size results in small shaping error. When the relationship between the size of input and output beam meets $R_0 \geq 1.3 w_0$, the shaping error approaches its minimum value. The lens with focal length $2m$ is used to focus the output and target beam. The power-in-the-bucket (PIB) curves of far field irradiance of the output and target beam are shown in Fig. 4(b). When the relationship between input and target beam meets $R_0 < 1.3 w_0$, the power in the main lobe of the far field irradiance of the output beam is smaller than that of the target beam. When the relationship between input and target beam meets $R_0 \geq 1.3 w_0$, the power in the main lobe of the far field irradiance of the output beam is larger than that of the target beam.

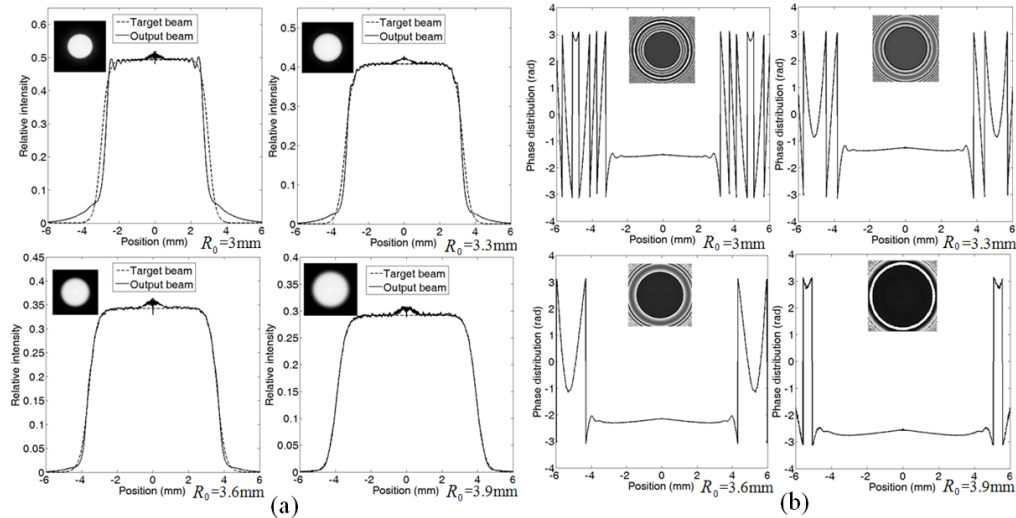Fig. 2. Phase distributions of dual aspheric lenses, (a) aspheric lens 1, (b) aspheric lens 2.

Fig. 3. The change of irradiance and phase distribution of the output beam along with target beam size (R_0), (a) irradiance distribution, (b) phase distribution.
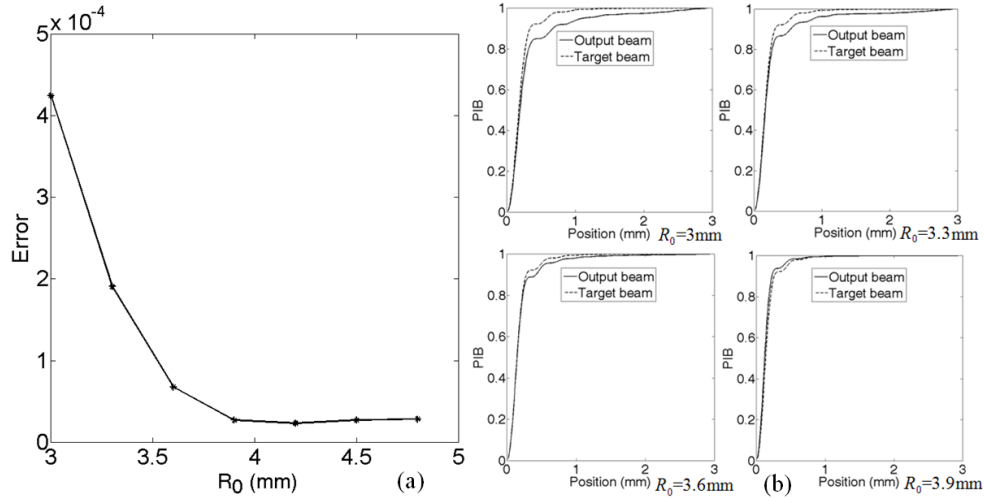
Fig. 4. The change of shaping error and PIB curve along with target beam size (R_0), (a) shaping error, (b) PIB curve.

2.2 Influence of the target beam order (β)

The parameters are $w_0 = 3mm$, $R_0 = 3.3mm$, $d = 350mm$, $n = 1.45$, and $\lambda = 1064nm$. The changes of phase distributions of dual aspheric lenses along with beam order (β) are shown in Fig. 5. It is found that the increase of target beam order (β) results in the increase of the difference between center and edge of the dual aspheric lenses. However, increase of the target beam order (β) has little influence on the movement of point of inflexion in phase distribution curve. The corresponding irradiance and phase distributions of the output beam are shown in Figs. 6(a) and 6(b). The change of the shaping error along with the increase of the beam order (β) is shown in Fig. 7. It can be found that the increase of beam order (β) results in larger difference between output and target beam. The flat area of the output beam decreases along with the increase of the beam order. The reason can be concluded as that the increase of the beam order results in slight decrease of the beam size. Compared with the numerical analysis mentioned in section 2.1, the influence of target beam size on beam shaping is much larger than that of the target beam order, so the shaping error of the conventional Galilean shaping system is mainly caused by the beam size.
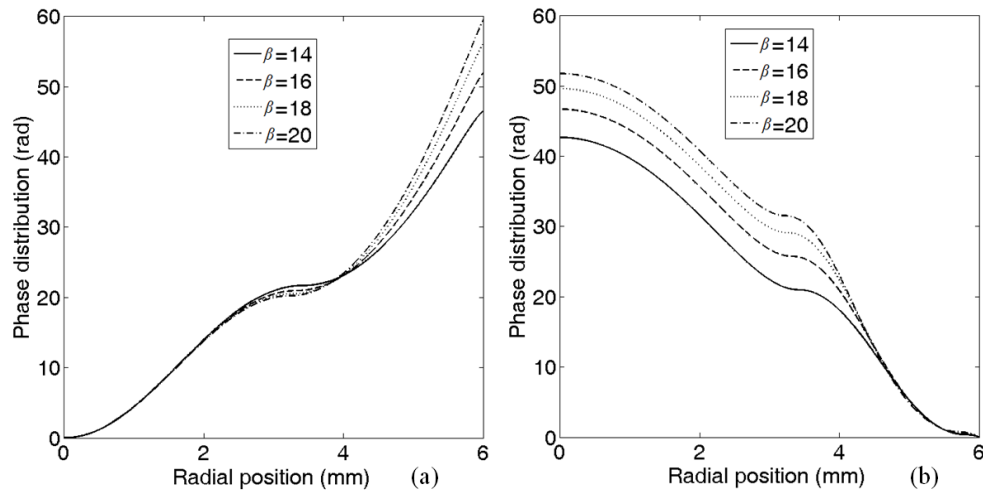

Fig. 5. Phase distributions of the dual aspheric lenses, (a) aspheric lens 1, (b) aspheric lens 2.
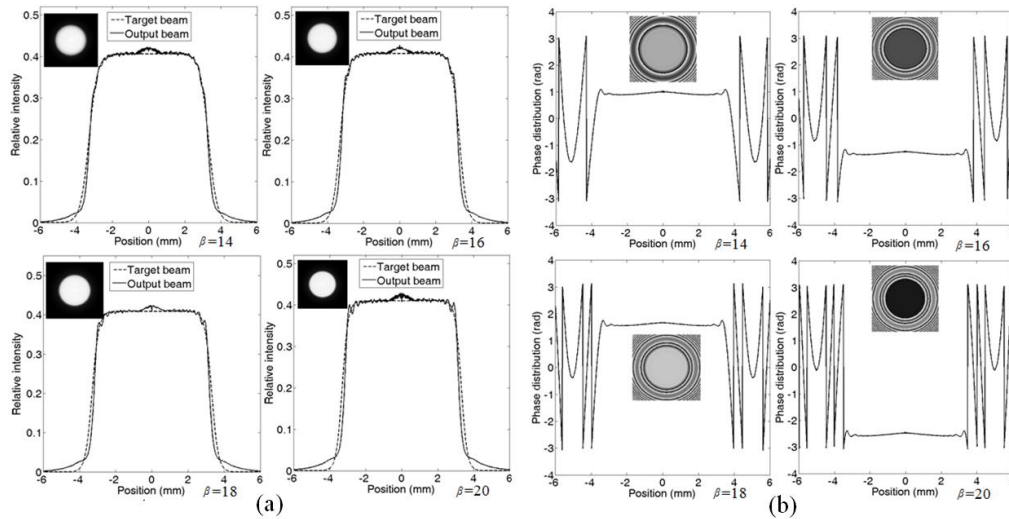
Fig. 6. The change of irradiance and phase distribution of the output beam along with target beam order (β), (a) irradiance distribution, (b) phase distribution.
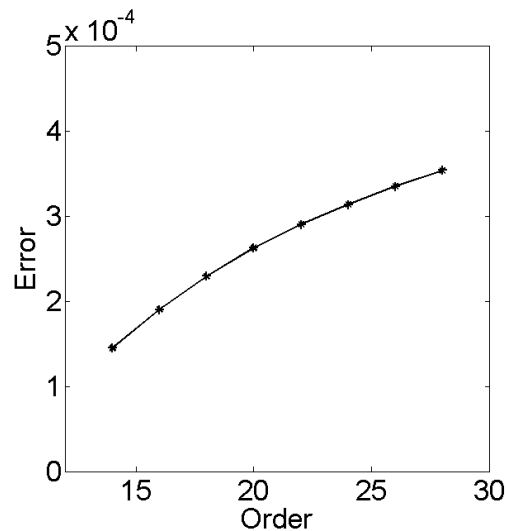

Fig. 7. The change of shaping error along with target beam order (β).

3. Improvement of the Galilean beam shaping system

From the analysis mentioned above, we can draw a conclusion that the Galilean beam shaping system can only suitable for magnifying beam shaping. The function of a beam shaper is to uniformly redistribute the input beam energy over the designated output surface area. The magnification for rays near the axis is larger than that entering near the edge. Consequently, rays at smaller radial position r on the front surface tend to defocus more than those at larger r, ending at with larger value of R on the rear surface. It can be thought that there must be a point where the input ray passes straight through the optical material and reach the rear surface without any focusing and defocusing. The conventional Galilean beam shaping system is assumed that the relationship between input radial position r and output radial position R is $R \geq r$. The configuration is shown in Fig. 8(a). In this configuration, only at position a (on axis), R equals to r. We regard this configuration as the magnifying system. The design

principle of the conventional Galilean beam shaping system is based on this configuration. However, many applications cannot meet this condition. For example, in the configuration shown in Fig. 8(b), the size of the target beam is smaller than that of the input beam. R equals to r at positions a, b, and c. At the region between a and b or between a and c, $R \geq r$ (corresponding to magnifying beam shaping system); at the region between b and the edge or between c and the edge, $R \leq r$ (corresponding to demagnifying beam shaping system). We regard this beam shaping system is demagnifying shaping system as a whole. According to the working principle, the design principle of conventional Galilean beam shaping system can only work well for the condition that there is no other straight ray except the center ray on optical axis where $r = R = 0$.
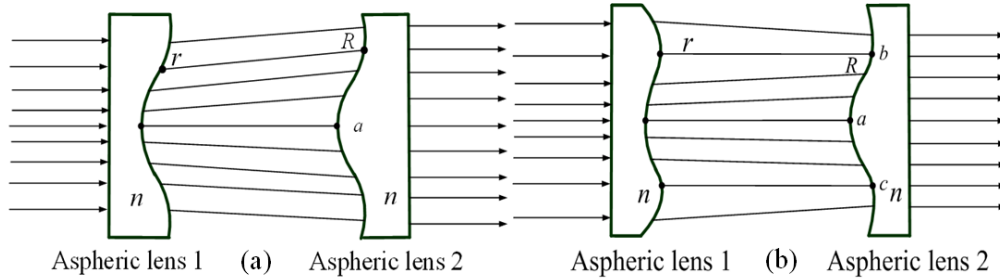

Fig. 8. Configuration of the Galilean beam shaping system, (a) magnifying beam shaping system, (b) demagnifying beam shaping system consisted of one magnifying and one demagnifying systems.

To overcome the shortcomings mentioned above, we regard the Galilean beam shaping system as the combination of magnifying and demagnifying beam shaping system. We deduce the relationship between radial position and surface distribution of the improved Galilean beam shaping system. The surface distributions of the improved Galilean beam shaping system, which contains only one magnifying and demagnifying systems, can be represented as

$$
\left\{
\begin{aligned}
z(r_1) &= \int_0^{r_1} \left\{ (n^2 - 1) + \left[\frac{(n-1)d}{h(x) - x} \right]^2 \right\}^{-1/2} dx & 0 < r_1 < h_1 \\
z(r_2) &= z(h_1) - \int_{h_1}^{r_2} \left\{ (n^2 - 1) + \left[\frac{(n-1)d}{h(x) - x} \right]^2 \right\}^{-1/2} dx & h_1 < r_2 < h_2
\end{aligned}
\right. \tag{8}
$$

and

$$
\left\{
\begin{aligned}
Z(R_1) &= \int_0^{R_1} \left\{ (n^2 - 1) + \left[\frac{(n-1)d}{h^{-1}(x) - x} \right]^2 \right\}^{-1/2} dx & 0 < R_1 < H_1 \\
Z(R_2) &= Z(H_1) - \int_{H_1}^{R_2} \left\{ (n^2 - 1) + \left[\frac{(n-1)d}{h^{-1}(x) - x} \right]^2 \right\}^{-1/2} dx & H_1 < R_1 < H_2
\end{aligned}
\right. , \tag{9}
$$

where h_1 is the position of point of inflexion on the phase distribution curve of the first aspheric lens. H_1 is the position of point of inflexion on the phase distribution curve of the second aspheric lens. $z(h_1)$ is the sag of the first aspheric lens at position h_1. $Z(H_1)$ is the sag of the second aspheric lens at position H_1. According to Fourier Optics, the relationships between phase distribution and radial position can be shown in Eqs. (10) and (11).

$$f_{phase1}(r) = \frac{2\pi\left[z_{\max} - z(r) + nz(r)\right]}{\lambda} \tag{10}$$

and

$$f_{phase2}(R) = \frac{2\pi\left[nZ_{\max} - nZ(R) + Z(R)\right]}{\lambda}, \tag{11}$$

where $f_{phase1}(r)$ and $f_{phase2}(R)$ are the phase distributions of dual aspheric lenses, $z_{\max}$ and $Z_{\max}$ are the maximum values of sag distributions of the first and second aspheric lens. Based on the same principle, we can also deduce the surface and phase distribution of more complicated beam shaping system, which contains many magnifying and demagnifying beam shaping systems.
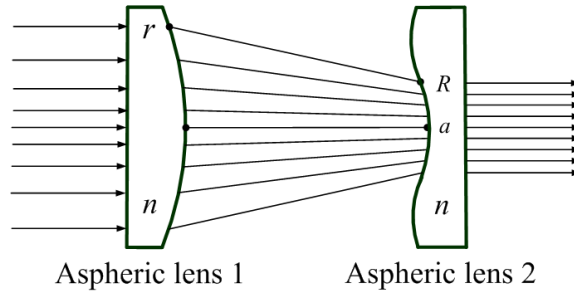

Fig. 9. Configuration of the demagnifying beam shaping system consisted of only one demagnifying system.

In other application, which is shown in Fig. 9, the region of $R>r$ is much smaller than the region of $R\leq r$, so the shaping system can be regarded as the combination of only one demagnifying beam shaping system. In this case, the technique proposed in this paper is still valid. The point of the inflexion is proximate the optical axis, which can be represented as $h_1 = H_1 \approx 0$. The detailed analysis will be given in the following paragraphs. In addition, we find that the proposed technique is also valid for solving the surface profile for the magnifying beam shaping system shown in Fig. 8(a). In such a case, the point of inflexion h_1 and H_1 meets $h_1 = H_1 \geq h_2$ or $h_1 = H_1 \geq H_2$, so the magnifying beam shaping system shown in Fig. 8(a) and the demagnifying beam shaping system shown in Fig. 9 can be regarded as the two special cases of the improved Galilean beam shaping system shown in Fig. 8(b).

Larger target beam order (β) and smaller target beam size (R_0) result in larger difference between the output beam and target beam, so we choose the target beam with large beam order and small beam size for analysis. The parameters of input and target beams are chosen as $w_0 = 3mm$, $R_0 = 3mm$, $\beta = 20$, $d = 350mm$, $n = 1.45$, $\lambda = 1064nm$. From Eqs. (8)–(11), the surface and phase distributions of dual aspheric lenses are calculated and shown in Figs. 10(a) and 10(b). It is found that the surface and phase distributions of the improved Galilean beam shaping system are not the same as that of the conventional Galilean beam shaping system. The edge's surface and phase distributions of the improved Galilean beam shaping system are smaller than that of point of inflexion; on the contrary, the edge's surface and phase distributions of the conventional Galilean beam shaping system are larger than that of point of inflexion. That is the reason that results in the difference between the output beam and the target beam in conventional Galilean beam shaping system. The irradiance and phase distributions of the input Gaussian beam passing through the improved Galilean beam shaping system are shown in Figs. 11(a) and 11(b). The near field irradiance distribution of the output beam is coincident with the target beam and the corresponding phase distribution is maintained. The shaping precision is much larger than that of the conventional Galilean beam shaping system.
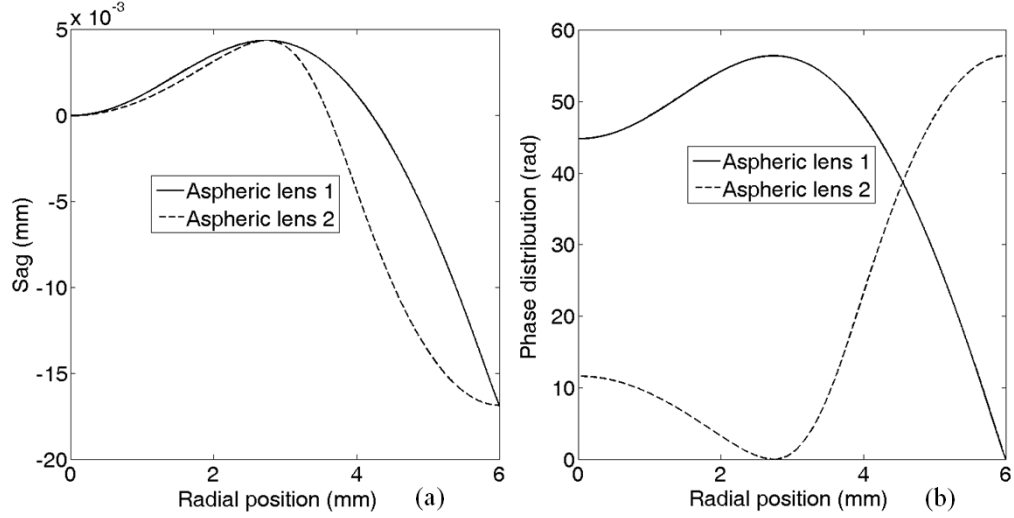
Fig. 10. Surface and phase distributions of the improved Galilean beam shaping system, (a) surface distributions, (b) phase distributions.
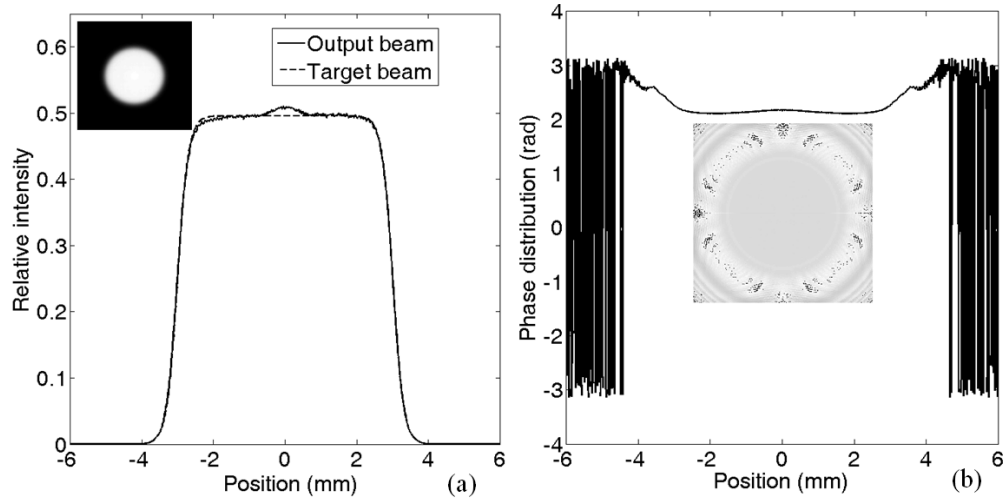

Fig. 11. Irradiance and phase distributions of the output beam, (a) Irradiance distribution, (b) phase distribution.

The uniformity and efficiency are usually used to evaluate the output beam. The relative *rms* variation of the output beam and conversion efficiency can be given by [2]

$$SE = \frac{a\left\{\int_0^a \left[P_{output}(r) - \frac{2}{a^2}\int_0^a P_{output}(r)rdr\right]^2 rdr\right\}^{\frac{1}{2}}}{\sqrt{2}\int_0^a P_{output}(r)rdr} \tag{12}$$

and

$$\eta = \frac{2\pi \int_0^a P_{output}(r)rdr}{W_{input}}, \tag{13}$$

where *SE* is the relative *rms* variation of the output flattop beam. *a* is the radius of interested region. W_{input} is the power of the input beam. From the irradiance distribution shown in Fig. 11(a), we define a region of interest centered on the beam axis and compute the sum, average and variance of the values within the region. By varying the region, we deduce the relationship between variance and the efficiency. Figure 12 shows the relative intensity variation as well as the results of the target flattop beam. From Fig. 12, it is found that approximately 80% of the total power is contained in the flattop region having less than 6% *rms* irradiance variation.

The lens with focal length 2*m* is used to focus the output beam. The far field irradiance distribution of the output beam is shown in Fig. 13. It is found that the far field irradiance of the output beam is coincident with the far field irradiance of the target beam, which shows that output beam is well compensated. The irradiance distributions of the output beam along with the propagation distance are shown in Fig. 14(a). The corresponding result of the flattop beam generated by conventional Galilean beam shaping system is shown in Fig. 14(b). The intensity profile remains a useful flattop shape without significant diffraction peaks for a propagation distance of more than 1.2*m*. However, the propagation distance of the flattop beam generated by the conventional Galilean beam shaping system is less than 0.4*m*. The propagation performance has been greatly improved.
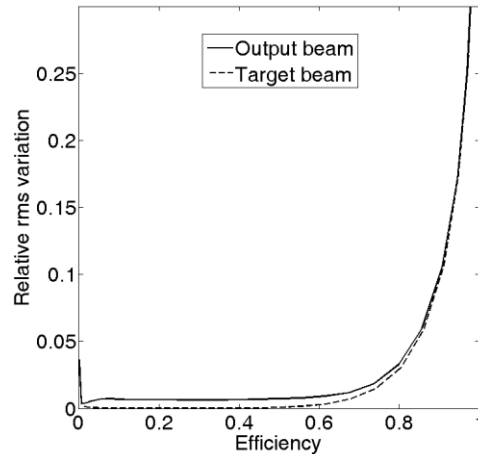

Fig. 12. Dependence of *rms* intensity variation of the output beam on efficiency compared with that of the target beam.
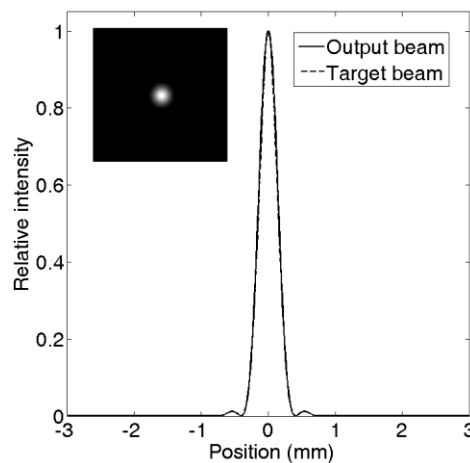

Fig. 13. Far field irradiance distributions of the output and target beam.
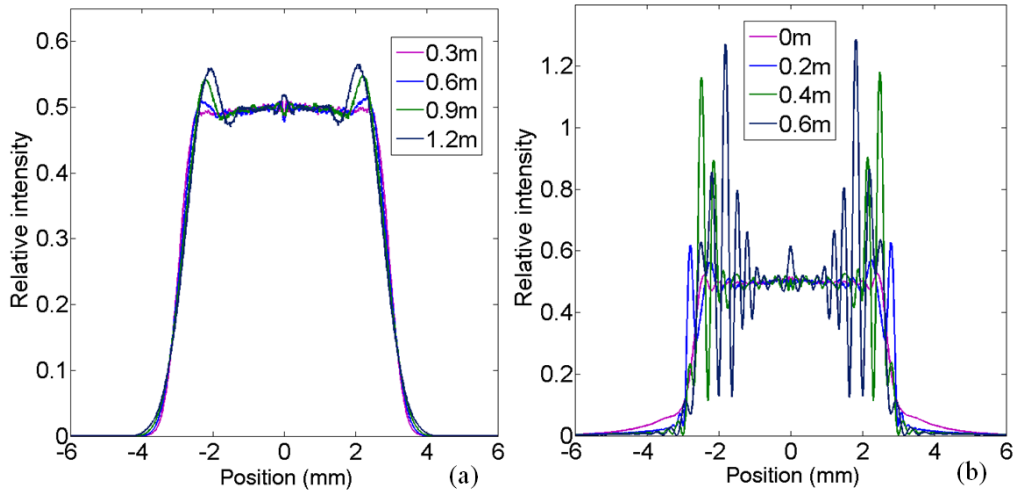
Fig. 14. The change of the irradiance distribution of the output beam along with the propagation distance, (a) generated by the improved Galilean beam shaping system, (b) generated by the conventional Galilean beam shaping system.

According to Eq. (7), we study the influences of beam size (R_0) and beam order (β) of the target beam on the improved Galilean beam shaping system. The parameters $w_0 = 3mm$, $\beta = 16$, $d = 350mm$, $n = 1.45$, $\lambda = 1064nm$ and the parameters $w_0 = 3mm$, $R_0 = 3.3mm$, $d = 350mm$, $n = 1.45$, $\lambda = 1064nm$ are chosen respectively in the numerical analysis. The changes of the shaping error along with the size and order of the target beam are shown in Figs. 15(a) and 15(b). From Figs. 15(a) and 15(b), we can see that the decrease of the beam size (R_0) and increase of the beam order (β) results in larger shaping error. However, the shaping error of the improved Galilean beam shaping system is much smaller than that of the conventional Galilean beam shaping system. The restriction of beam size on Galilean beam shaping system has been greatly reduced.
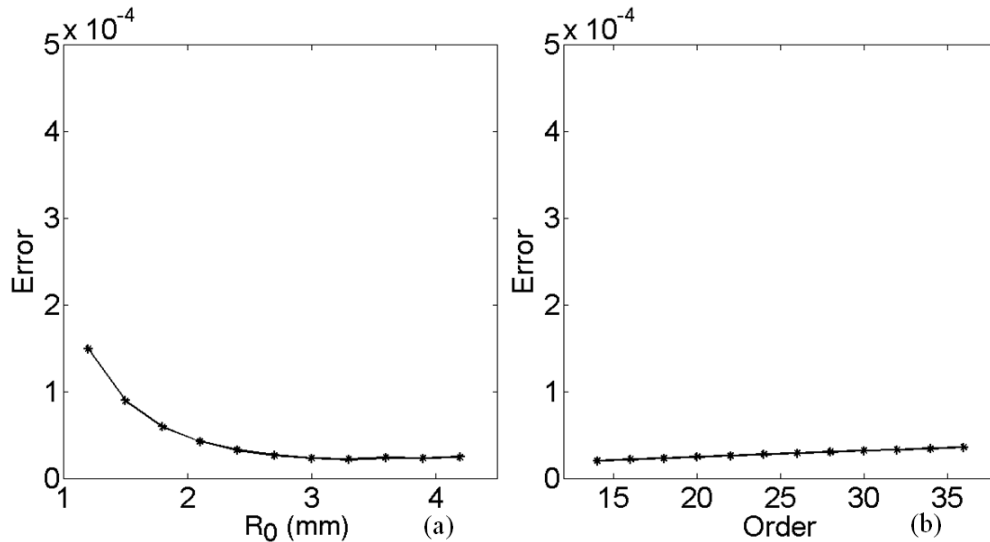

Fig. 15. The change of shaping error along with beam size (R_0) and beam order (β), (a) with beam size (R_0), (b) with beam order (β).

Based on the energy conservation, we can find that if the target beam size meets $R_0 \leq 1.8mm$, the point of inflexion $h_1 = H_1 \leq 10um$. The magnifying region is much smaller than

the demagnifying region. The Galilean beam shaping system can be regarded as the combination of only one demagnifying beam shaping system. The parameters $w_0 = 3mm$, $R_0 = 0.9mm$, $\beta = 16$, $d = 350mm$, $n = 1.45$, and $\lambda = 1064nm$ are chosen to investigate the performance of Galilean beam shaping system consisted of only one demagnifying beam shaping system. The irradiance and phase distribution of the output beam are shown in Figs. 16(a), 16(b) and 16(c). From Figs. 16(a), 16(b) and 16(c), we can see that the flattop beam with plane phase distribution is realized by the improved Galilean beam shaping system. The far field irradiance distribution of the output beam is nearly identical to the target beam. However, there exist difference between the near field irradiance distributions of the output beam and the target beam near the optical axis. It can be concluded that the technique proposed in this paper is suitable for the beam shaping system consisted of only one demagnifying beam shaping system. The error is just become larger with the decrease of the target beam size.
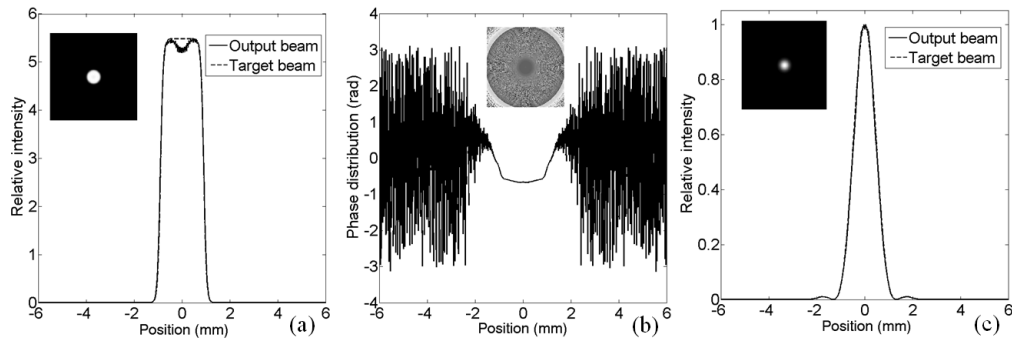

Fig. 16. The irradiance and phase distribution of the output beam, (a) near field irradiance distribution, (b) phase distribution, (c) far field irradiance distribution.

5. Conclusions

The improvement of the conventional Galilean refractive beam shaping system has been proposed and demonstrated. According to the detailed studies on the conventional Galilean beam shaping system, it is found that the conventional Galilean beam shaping system can only work well for the magnifying beam shaping. For the improved Galilean beam shaping system, the shaper is regarded as the combination of magnifying and demagnifying beam shaping system. The transformation of Gaussian beam into high order Fermi-Dirac profile flattop beam is used to verify the feasibility of the improvement. The numerical simulation results show that the output beam is nearly coincident with the target beam and the phase distribution of the output beam is maintained. Approximately 80% of the power is enclosed in a region with less than 6% *rms* power variation. The flattop beam retains a useful flat-top irradiance distribution without significant diffraction peaks for a working distance of more than $1.2m$. However, the propagation distance of the flattop beam generated by the conventional Galilean beam shaping system is less than $0.4m$. The propagation performance has been greatly improved. The change of the shaping error of the target beam size and beam order on the improved Galilean beam shaping system has been investigated in detail. The restriction of beam size on beam shaping system has been greatly reduced. The transformation of input beam with arbitrary beam size into output beam with arbitrary beam size can be realized by this improved Galilean beam shaping system. This study provides useful guidelines to the improvement of the conventional refractive beam shaping system.